PCCP

Accepted Manuscript

ROYAL SOCIETY OF CHEMISTRY

www.rsc.org/pccp

Journal Name

ARTICLE TYPE

Cite this: DOI: 10.1039/xxxxxxxxxx

Received Date
Accepted Date

DOI: 10.1039/xxxxxxxxxx

www.rsc.org/journalname

Nuclear Quantum Fluctuations in Ice I$_h$

Pedro Augusto Franco Pinheiro Moreira[a*] **and Maurice de Koning**[b*]

We discuss the role of nuclear quantum fluctuations in ice I$_h$, focusing on the hydrogen-bond (HB) structure and molecular dipole-moment distribution. For this purpose we carry out DFT-based first-principles molecular dynamics and path-integral molecular dynamics simulations at $T = 100K$. We analyze the HB structure in terms of a set of parameters previously employed to characterize molecular structure in the liquid phase and compute molecular dipole moments using maximally-localized Wannier functions. The results show that the protons experience very large digressions driven by quantum fluctuations, accompanied by major rearrangements in the electronic density. As a result of these protonic quantum fluctuations the molecular dipole-moment distribution is substantially broadened as well as shifted to a larger mean value when compared to the results obtained when such fluctuations are neglected. In terms of the dielectric constants, the reconciliation of the greater mean dipole moment with experimental indications that the dielectric constant of H_2O ice is lower than that of D_2O ice would indicate that the topology of the HB network is sensitive to protonic quantum fluctuations.

---

[a] *Departamento de Física, UFSCar, Rodovia Washington Luiz, km 235, CP 676, 13565-905, São Carlos-SP, Brazil. Fax: +55 16 3361-4835; Tel: +55 16 3351-8223; E-mail: pmoreira@ufscar.br*

[b] *Instituto de Física 'Gleb Wataghin', Universidade Estadual de Campinas, 13083-859, Campinas-SP, Brazil. E-mail: dekoning@ifi.unicamp.br*

1 Introduction

Despite the simplicity of the isolated water molecule, its condensed phases display an astonishing richness of properties that is central to many different areas of research, ranging from (bio)chemistry and condensed-matter physics to atmospheric science and geophysics. Yet, despite many decades of intense experimental and theoretical investigation, many of these remain poorly understood.[1,2]

Considering the most common crystalline phase of water, the proton disordered hexagonal ice I_h, one of the issues that has been subject of debate concerns its dielectric properties.[2] For instance, in addition to the debate regarding the anisotropy of ice's dielectric constants,[2–7] the characterization of their temperature dependence in terms of a Curie-Weiss law[2,8] and its corresponding interpretation in terms of the ice I_h to ice XI ferroelectric ordering transition near $T = 72K$ continues to be a subject of investigation.[6,7]

Computational modeling has played an increasingly important role in clarifying the dielectric properties of ice I_h.[6,7,9–15] Employing semi-empirical force fields of different degrees of sophistication[6] or density-functional theory (DFT) approaches based on a variety of functionals[7], the dielectric properties are usually determined using well-known fluctuation relations of the form[6]

$$\varepsilon_s - \varepsilon_\infty = \frac{4\pi}{3k_BTV}\langle \vec{P}\cdot\vec{P}\rangle \tag{1}$$

for the static dielectric constant ε_s, with ε_∞ the infinite-frequency dielectric constant, k_B Boltzmann's constant, T the absolute temperature, $\vec{P}$ the total polarization vector of the system contained in a volume V and the angular brackets denote an ensemble average, or, more generally,

$$\varepsilon_{ij} - \varepsilon_\infty\delta_{ij} = \frac{4\pi}{k_BTV}\langle P_iP_j\rangle \tag{2}$$

for the full dielectric tensor, with δ_{ij} the Kronecker delta and $P_{i,j}$ components of $\vec{P}$. The above expressions represent the fact that the dielectric properties are determined by the "width" of the total-dipole-moment distribution, describing the magnitude of its equilibrium fluctuations. For the condensed phases of water the total dipole moment of a system is given by the sum of N molecular dipole moments, i.e., $\vec{P} = \sum_{i=1}^{N}\vec{\mu}_i$, with $\vec{\mu}_i$ the dipole moment vector of molecule i. Taking into account the width of the molecular dipole-moment distribution and assuming that fluctuations on different molecules are not correlated, ε_s becomes

$$\varepsilon_s - \varepsilon_\infty = \frac{4\pi N}{3k_BTV}\left(\langle(\mu - \langle\mu\rangle)^2\rangle + \langle\mu\rangle^2 G\right), \tag{3}$$

with G the geometrical factor[16]

$$G \equiv \frac{\langle(\sum_{i=1}^{N}\vec{u}_i)^2\rangle}{N} \tag{4}$$

in which $\vec{u}_i$ is the unit vector describing the direction of molecular dipole moment $\vec{\mu}_i$.[6]

The relevant fluctuations involved in the values of the dielectric constants are composed of two contributions: (i) topological fluctuations and (ii) molecular dipolar variations within a given HB topology. The first incorporates the many possible hydrogen-bond (HB) topologies associated with the proton-disordered character of ice I_h consistent with the energy differences between the different configurations[17] and is encoded mainly in the factor G. The second concerns individual molecular dipole-moment variations, both in magnitude as well as in orientation, due to fluctuations of thermal and nuclear quantum-mechanical origin.

Proper quantification of these fluctuations, required to correctly evaluate the ensemble averages in Eqs. (1) and (2), is rather involved. The sampling of topological fluctuations has been achieved using Markov-chain Monte Carlo methods in which one particular realization of the HB network is transformed into another by finding closed loops of HBs and attempting to invert their orientation.[9–12] Combining this approach with the sampling of molecular motion based on a description in terms of empirical force fields[6] or DFT calculations[7] then allows simultaneous access to topological and thermal fluctuations.

The role of quantum fluctuations in this context, however, has received much less attention. They are often regarded as relatively small,[7] but without providing a quantitative estimate. Following the pioneering *ab initio* Path-integral molecular dynamics (PIMD)[18] simulations by Chen *et al.* studying the structure of liquid water,[19] Morrone and Car considered molecular dipole-moment distributions for liquid water and also were the first to consider protonic quantum effects in ice I_h, but restricted their analysis for the latter to the proton-momentum distribution.[20] Several other studies have since shown that protonic quantum effects can be significant in the condensed phases of water.[21–27] In particular, Ceriotti *et al.*[24] have recently shown that the HB structure in liquid water is significantly affected, for instance leading to the occurrence of autoprotolysis events that are entirely absent when the protons are treated as classical particles. Furthermore, for the case ice of I_h, very recent PIMD simulations have shown that coherent proton-tunneling effects may actually occur more frequently than previously thought.[25,26]

In the present paper we analyze the influence of protonic quantum fluctuations on the HB structure and molecular dipole-moment distribution in ice I_h and quantify their contribution to its dielectric properties. For this purpose we compare the results of DFT-based PIMD simulations to those obtained from standard first-principles MD calculations in which the protons are treated classically. In particular, we analyze the HB fluctuations in terms of the set of structural parameters used by Ceriotti *et al.* in their analysis of HBs in liquid water[24] All calculations are carried out at a temperature of 100 K, which is already close to ice $I_h \rightarrow XI$ ferroelectric ordering transition,[2] and for which converged PIMD results can be obtained using moderate numbers of replicas.

The remainder of the paper has been organized as follows. Section 2 summarizes the methodological and computational details of our calculations. We then report and discuss the obtained results in Section 3, followed by our conclusions in Section 4.

2 Methodology and Computational details

All the calculations are based on the proton-disordered, defect-free, 96-molecule periodic cell labeled $3\times2\times2$ as generated by

Hayward and Reimers[28], with the volume rescaled to the experimental a and c values at $T = 100$ K.[2] All first-principles MD and PIMD simulations were carried out using the CPMD package[29]. In the MD simulations treating the protons as classical particles, the electronic-structure problem was solved by converging the Kohn-Sham (KS) wavefunction at each step, using a plane-wave cutoff of 75 Ry, Γ-point Brillouin-zone sampling and Troullier-Martins norm-conserving pseudopotentials[30]. Most calculations were done using the PBE[31] approximation to the exchange-correlation (XC) functional, but to assess the sensitivity with respect to the used XC approximation a few MD calculations were also carried out to compute the dipole moment using the BLYP[32,33] functional. The Nosé-Hoover[34,35] scheme with a thermostat period of 10^{-2} ps was used to control the temperature and the corresponding equations of motion were integrated using a time step of $\Delta t = 0.1$ fs. Following initial equilibration for at least 1000 steps, statistics was gathered for another 10.000-20.000.

The DFT-based PIMD calculations were carried out using the Car-Parrinello approach,[36] with a fictitious electron mass of 0.1 a.m.u. and a time step of 0.075 fs. As for the case of the classical-proton simulations, the plane-wave cut-off was 75 Ry, Brillouin sampling was restricted to the Γ-point and Troullier-Martins norm-conserving pseudopotentials were employed. Because of the computational cost only the PBE approximation for the exchange-correlation functional was used in the PIMD calculations. Indeed, Ceriotti *et al.* have shown that the quantum fluctuations captured in the PIMD simulations are rather insensitive to the choice of XC functional because of the large energy scale associated with the zero-point motion in a water molecule.[24] Both the ions as well as the electrons were thermostatted using the massive Nosé-Hoover method,[37] with thermostat time constants of $10^{-}2$ and 3×10^{-3} ps for the ions and electrons, respectively, and the fictitious electronic temperature targeted at 8×10^{-3} K. The paths were discretized using 8, 16 and 32 replicas, respectively, and the normal-mode representation of the path-integral propagator was used. After equilibration of about 10.000 time steps, statistics was gathered for more than 80.000 time steps, sampling path configurations every 25th step.

To analyze the HB structure we use the same structural order parameters as those reported by Ceriotti *et al.*[24]. Consider Fig. 1, which shows a schematic representation of the structures of two water molecules that are linked by a hydrogen bond. The proton that links the two water molecules is denoted by H and the Wannier center associated with the covalent bond that binds it to the donor molecule with oxygen ion O is referred to as X. The acceptor molecule, centered on oxygen ion O', completes the HB through the lone pair orbital described by Wannier center X' As detailed by Ceriotti *et al.* it is useful to characterize the HB structure in terms of the proton-transfer coordinate $\nu \equiv d(O-H) - d(O'-H)$, with $d(A-B)$ representing the distance between A and B, the angle $\alpha \equiv \widehat{O'OH}$, and the distances $d(O-O')$, $d(O-X)$ and $d(O'-X')$. The parameter ν measures the position of the HB proton relative to the two oxygen ions involved. Negative values imply that it is closest to its "own" donor ion, whereas positive values indicate that it has moved into the vicinity of the acceptor oxygen, signaling the occurrence of a geometric autoprotolysis event.

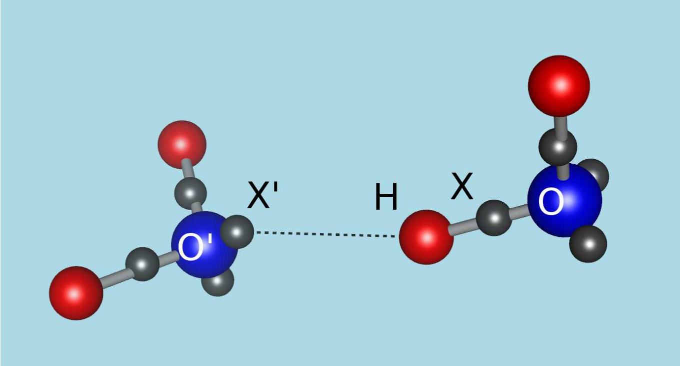

Fig. 1 Schematic representation of two water molecules linked by a hydrogen bond. Blue, red and grey spheres represent oxygen ions, protons and Wannier centers respectively. Wannier center associated with the covalent bond that binds the donating proton, H, to oxygen ion O is denoted with X. The Wannier center that serves as proton acceptor on the other water molecule, with oxygen ion O' is referred to as X'.

The molecular dipole moments are computed from the KS electronic structures using maximally localized Wannier functions (MLWF).[38] The dipole moment vector of a given water molecule is then computed as

$$\vec{\mu} = 6e\vec{R}_O + e\vec{R}_{H_1} + e\vec{R}_{H_2} - 2e\sum_{n=1}^{4}\langle R_n \mid \vec{r} \mid R_n\rangle, \tag{5}$$

with e the magnitude of the electron charge, $\vec{R}_O$, $\vec{R}_{H_1}$ and $\vec{R}_{H_2}$ the position vectors of the oxygen ion and the 2 protons, respectively, and the matrix elements representing the Wannier centers of the relevant KS orbitals. For the Car-Parrinello PIMD simulations the Wannier centers were determined after an *a posteriori* optimization of the KS orbitals for each configuration.

3 Results and discussion

First we examine the differences between the HB structure for the cases of classical ions and the situation in which they are treated quantum-mechanically within the PIMD framework using 32 replicas. Fig. 2 a) and b) show the joint probability density $P(\nu, \cos\alpha)$ of observing a HB $O-H\cdots O'$ with a geometry characterized by the order parameters ν and cos α for the cases of classical and quantum-mechanical nuclei, respectively. In the static relaxed ice I_h structure the values of ν and cos α are very close to -0.75 Å and 1, respectively. Fig. 2a) shows the influence of thermal fluctuations on these values and it can be seen that in this case the deviations from the static values are quite small. In particular, the parameter ν never comes close to zero, meaning that the protons remain covalently bonded to their host molecule at all times. When including quantum effects this changes significantly, as can be seen in Fig. 2b). The fluctuations associated with the protonic zero-point motion lead to a very broad probability distribution, with angular deviations of as much as 35° and, more importantly, values of ν that substantially exceed zero. The latter implies that, as was already observed for liquid water,[24] the probability to observe short-lived large proton excursions that geometrically constitute autoprotolysis is appreciable. Indeed, these

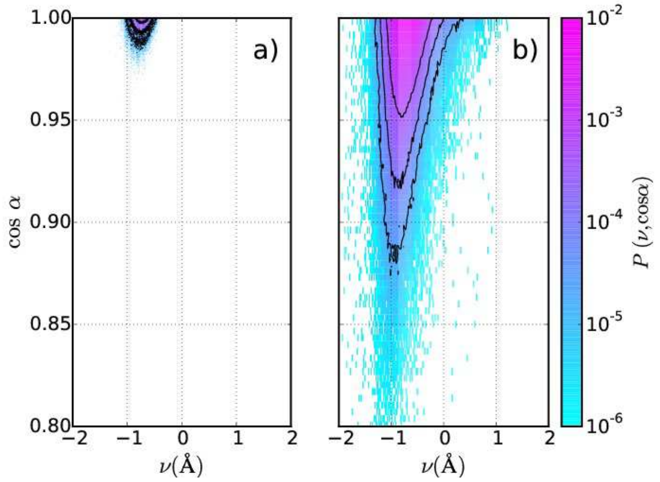

Fig. 2 Joint probability density $P(\nu,\cos\alpha)$ to observe HB structure O − H$\cdots$O′ in ice I$_h$ at $T = 100\ K$ for the cases in which the ions are treated (a) classically, and (b) quantum-mechanically using PIMD with 32 replicas. Black lines represent iso-probability contours at 5×10^{-4}, 1×10^{-4} and 2×10^{-5}.

large deviations may be closely related to the coherent proton-tunneling effects reported recently.[25,26]

Similarly, Fig. 3 shows the joint probability density to observe a HB with particular values of ν and $d(OO')$. As in Fig. 2, the distribution of ν values is greatly broadened by the protonic quantum effects. On the other hand, as expected given the comparatively large mass of the oxygen nuclei, the range of observed values for the oxygen-oxygen distance $d(O-O')$ is hardly affected by the quantum nuclear effects.

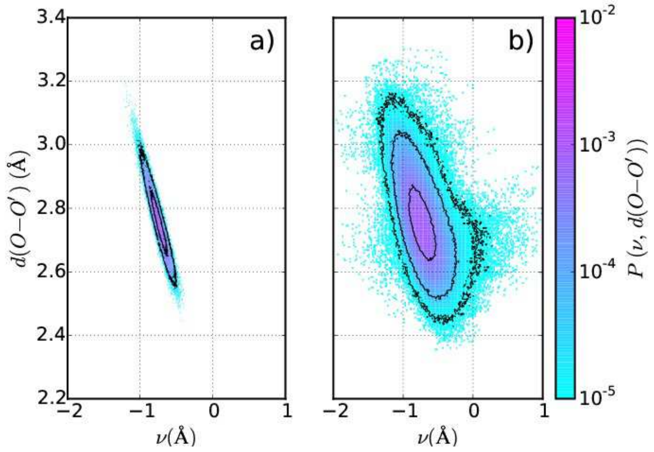

Fig. 3 Joint probability density $P(\nu,\ d(O-O'))$ for the cases in which the ions are treated (a) classically, and (b) quantum-mechanically using PIMD with 32 replicas. Black lines represent iso-probability contours at 5×10^{-6}, 5×10^{-5} and 5×10^{-4}.

The protonic quantum fluctuations also directly affect the electronic density of the water molecules. This can be seen in Fig. 4, which shows the joint probability densities $P(\nu,\ d)$, with d representing the distance between the donor oxygen and the bonding Wannier center, $d(O-X)$, or the distance between the acceptor oxygen and the lone-pair Wannier center, $d(O-X')$, respectively. While both distributions are entirely separated in the classical case, the protonic quantum fluctuations characterized by positive values of ν are accompanied by cross-over events in which covalent Wannier centers turns into a lone-pair centers and vice-versa, giving a distinct overlap between $P(\nu,\ d(O-X))$ and $P(\nu,\ d(O-X'))$. This shows that the large digressions driven by quantum fluctuations are also accompanied by significant rearrangements in the electronic density.

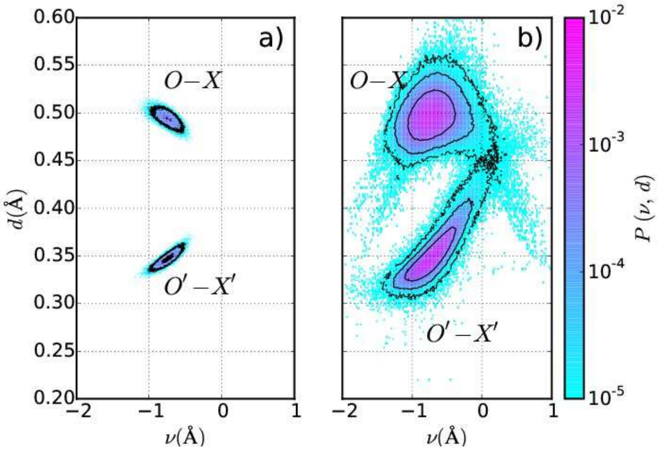

Fig. 4 Joint probability densities $P(\nu,\ d)$, with $d = d(O-X)$ or $d(O-X')$, for the cases in which the ions are treated (a) classically, and (b) quantum-mechanically using PIMD with 32 replicas. Black lines represent iso-probability contours at 5×10^{-6}, 5×10^{-5} and 5×10^{-4}.

To assess the total fraction of geometric autoprotolysis configurations we analyze the probability distributions of the transfer coordinate $P(\nu)$ shown in Fig. 5. While in the classical simulation not a single configuration with $\nu > 0$ was observed, the case in

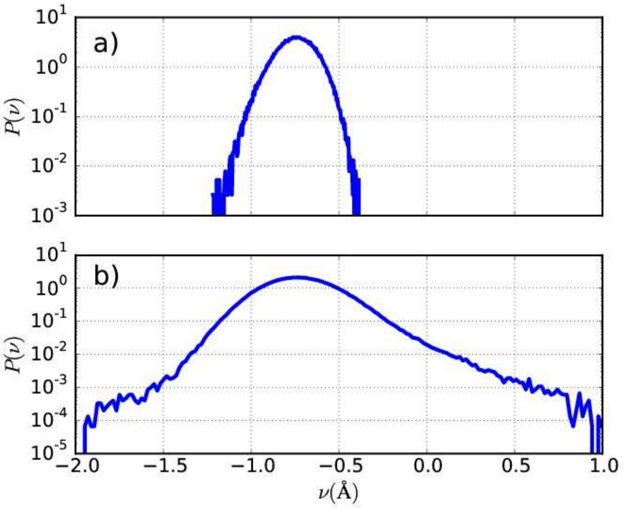

Fig. 5 Probability density $P(\nu)$ for the cases in which the ions are treated (a) classically, and (b) quantum-mechanically using PIMD with 32 replicas.

which the nuclei are treated quantum-mechanically reveals a significant number of such events. Numerically integrating the probability density in Fig. 5 b) for $\nu > 0$ gives a fraction of $\approx 3 \times 10^{-3}$, which is of the same order of magnitude as that found for liquid water.[24]

We now turn to the influence of the quantum fluctuations on the molecular dipole-moment distribution, which is controlled by the intra-molecular structure parameters such as the internal angle and the covalent O-H distance, as well by as the positions of the Wannier centers associated with the lone pairs and the covalent bonds. The distributions of these parameters for the cases of classical and quantum nuclei are shown in Fig. 6. For all parameters the quantum-mechanical treatment of the nuclei leads to distributions that are significantly broadened compared to the case of classical nuclei, in particular for the internal angle θ and the O-H distance. Considering the average values, however, both types of description give results that are essentially equal, with the exception of the covalent O-H distance, as can be seen Table 1. When taking into account the protonic quantum fluctuations, it is $\sim 3\%$ larger compared to the classical description. This result is not expected to change dramatically when a different XC functional is used. First, as mentioned before, Ceriotti *et al.*[24] have shown that the protonic quantum digressions are relatively insensitive to the chosen functional. Second, the same appears to be the case for the O-H in absence of protonic quantum fluctuations. To assess this sensitivity we carried out a first-principles MD simulation using the BLYP functional for ice I_h at $T = 100K$ and measured a mean O-H distance of 1.002 Å compared to a value of 1.007 Å for the PBE functional.

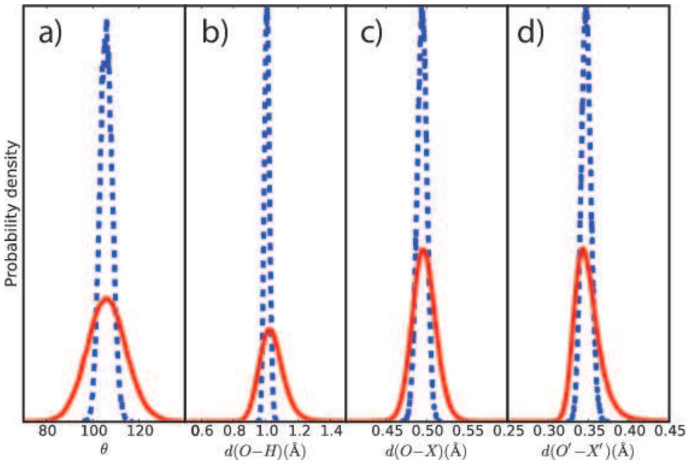

Fig. 6 Distributions of (a) the internal molecular angle θ, (b) covalent O-H distance, (c) covalent Wannier center distance $O-X$ and (d) lone-pair Wannier center distance $O'-X'$ for the cases in which the ions are treated classically (dashed line), and quantum-mechanically using PIMD with 32 replicas (full line).

The molecular dipole-moment distributions are shown in Fig. 7 a). In addition to the broadening, the inclusion of quantum fluctuations using 32 replicas leads to an average molecular dipole moment of $(3.56 \pm 0.01\ D)$, which is expected to be close to the result to be obtained for fully replica-converged PIMD simulations, as shown in the convergence sequence of Fig. 7b). This value is $\sim 4\%$ larger than that obtained for classical nuclei and, considering the molecular-structure parameters in Table 1, this difference is mainly due to the increased covalent O-H distance.

	Classical	PIMD
$\langle\theta\rangle$ (degrees)	105.76 ± 0.01	105.61 ± 0.02
$\langle d(O-H)\rangle$ (Å)	1.0072 ± 0.0002	1.030 ± 0.003
$\langle d(O-X)\rangle$ (Å)	0.494 ± 0.001	0.50 ± 0.01
$\langle d(O'-X')\rangle$ (Å)	0.347 ± 0.001	0.35 ± 0.02
$\langle\mu\rangle$ (D)	3.413 ± 0.001	3.56 ± 0.01
$\langle\mu^2\rangle - \langle\mu\rangle^2$ (D^2)	0.02 ± 0.01	0.22 ± 0.01

Table 1 Mean values of the internal molecular angle θ, covalent O-H separation, covalent Wannier center distance $O-X$, lone-pair Wannier center distance $O'-X'$ and total dipole moment, as well as the variance in the dipole moment for the cases in which the ions are treated classically and quantum-mechanically using PIMD with 32 replicas. Error bars represent the standard deviations in the mean.

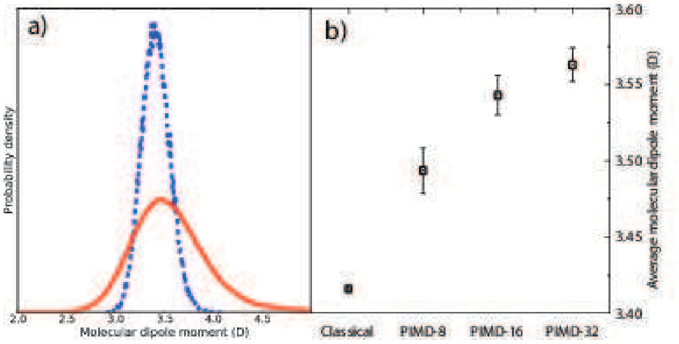

Fig. 7 (a) Distributions of the molecular dipole moment for the cases in which the ions are treated classically (dashed line), and quantum-mechanically using PIMD with 32 replicas (full line). (b) Average molecular dipole moment values obtained for classical nuclei as well as PIMD simulations based on 8, 16 and 32 replicas, respectively.

Interestingly, this difference does not occur for the case of liquid water, in which no significant deviations were found between the average dipole moments for classical and quantum descriptions of the nuclei.[20] As argued by Morrone and Car,[20] in the liquid phase the enhanced polarizability of molecules in the PIMD simulations is offset by the larger fraction of broken hydrogen bonds compared to the classical situation. In ice I_h all water molecules are fourfold coordinated regardless of the level of description, leading to a larger average dipole moment when nuclear quantum fluctuations are considered explicitly.

Finally, it is interesting to analyze the effects of an increased average dipole moment on the dielectric constants. If the geometrical factor G in Eq. (3) is unaffected by quantum effects, then the higher average molecular dipole moment for the case in which nuclear quantum effects are included would be expected to lead to a dielectric constant larger than that for classical nuclei. For instance, using the dipole-moment data in Table 1 in Eq. (3) and assuming $G \approx 2.55$[7], the dielectric constants for classical and quantum protons at a temperature of $100K$ would be $\varepsilon \approx 281$ and $\varepsilon_s \approx 308$, respectively. However, experimental data regarding the difference between the dielectric constants of H_2O ("more quantum") and D_2O ("less quantum") of Kawada[39] and Johari and Jones[40] seems to indicate otherwise, with the dielectric constants of the former being between 5% and 8% lower compared to those of the latter. Reconciliation of a higher average molecular dipole moment with a lower dielectric constant within the model of Eq. (3) would then suggest that protonic quantum effects reduce the G value compared to the case of classical nuclei. In other words, for the same Hamiltonian describing the energetics in ice I_h, the HB-network topology characteristics would be measurably different for the cases of classical and quantum protons, respectively. The quantification of such a difference would require a combined first-principles PIMD and HB-topology sampling approach of the kind used by Aragones *et al.*[6] and Schönherr *et al.*.[7]

4 Conclusions

We have conducted first-principles MD and PIMD calculations to study the influence of protonic quantum fluctuations on the HB structure and the molecular dipole-moment distribution in ice I_h at a temperature of $T = 100\ K$. The results show that the quantum fluctuations substantially affect the parameters that characterize the HB structure. In particular, the large digressions of the protonic positions give rise to a significant fraction of geometric autoprotolysis events, possibly involved in the coherent proton-tunneling phenomena reported recently.[25,26] Furthermore, the protonic quantum effects give rise to both a broadening as well as an increased mean value of the molecular dipole-moment distribution as compared to that obtained when considering the oxygen ions and the protons as classical particles. The greater average dipole-moment value is mostly due to the elongated O-H bond observed in the PIMD calculations. In terms of the dielectric constants, the reconciliation of the greater mean dipole moment with experimental indications that the dielectric constant of H_2O ice is lower than that of D_2O ice would indicate that the topology characteristics of the HB network, as encoded in the geometric factor G, are sensitive to protonic quantum fluctuations.

Acknowledgement

P.A.F.P.M. and M.K. acknowledge financial support from the Brazilian agencies Fapesp, Capes, CNPq and the Center for Computational Engineering and Sciences - Fapesp/Cepid no. 2013/08293-7.

References

1 D. Eisenberg and W. Kauzmann, *The structure and properties of water*, Oxford University Press, New York, 1969.

2 V. F. Petrenko and R. W. Whitworth, *Physics of ice*, Oxford University Press, New York, 1999.

3 S. Kawada, *J. Phys. Soc. Jpn.*, 1978, **44**, 1881–.

4 G. P. Johari and S. J. Jones, *J. Glaciology*, 1978, **21**, 259.

5 I. Takei and N. Maeno, *J. Phys. (Paris)*, 1987, **48**, C1, 121.

6 J. L. Aragones, L. G. MacDowell and C. Vega, *The Journal of Physical Chemistry A*, 2011, **115**, 5745–5758.

7 M. Schönherr, B. Slater, J. Hutter and J. VandeVondele, *J. Phys. Chem. B*, 2014, **118**, 590–596.

8 G. P. Johari and E. Whalley, *The Journal of Chemical Physics*, 1981, **75**, 1333–1340.

9 A. Rahman and F. H. Stillinger, *J. Chem. Phys.*, 1972, **57**, 4009–4017.

10 G. T. Barkema and J. de Boer, *J. Chem. Phys.*, 1993, **99**, 2059–2067.

11 V. Buch, P. Sandler and J. Sadlej, *J. Phys. Chem. B*, 1998, **102**, 8641–8653.

12 S. W. Rick and A. D. J. Haymet, *J. Chem. Phys.*, 2003, **118**, 9291–9296.

13 G. E. Lindberg and F. Wang, *J. Phys. Chem. B*, 2008, **112**, 6436–6441.

14 L. G. MacDowell, *J. Phys. Chem. B*, 2010, **114**, 6089.

15 A. J. Rusnak, E. R. Pinnick and F. Calderon, Camilo E. and, *J. Chem. Phys.*, 2012, **137**, 034510–7.

16 J. F. Nagle, *J. Chem. Phys.*, 1974, **61**, 883–888.

17 T. K. Hirsch and L. Ojamäe, *J. Phys. Chem. B*, 2004, **108**, 15856–15864.

18 D. Marx and J. Hütter, *Ab Initio Molecular Dynamics: Basic Theory and Advanced Methods*, Cambridge University Press, 2009.

19 B. Chen, I. Ivanov, M. L. Klein and M. Parrinello, *Phys. Rev. Lett.*, 2003, **91**, 215503.

20 J. A. Morrone and R. Car, *Phys. Rev. Lett.*, 2008, **101**, 017801.

21 R. Ramírez and C. P. Herrero, *The Journal of Chemical Physics*, 2010, **133**, 144511.

22 X.-Z. Li, B. Walker and A. Michaelides, *Proceedings of the National Academy of Sciences*, 2011, **108**, 6369–6373.

23 B. Pamuk, J. M. Soler, R. Ramírez, C. P. Herrero, P. W. Stephens, P. B. Allen and M.-V. Fernández-Serra, *Phys. Rev. Lett.*, 2012, **108**, 193003–.

24 M. Ceriotti, J. Cuny, M. Parrinello and D. E. Manolopoulos, *Proceedings of the National Academy of Sciences*, 2013, **110**, 15591–15596.

25 C. Drechsel-Grau and D. Marx, *Phys. Rev. Lett.*, 2014, **112**, 148302.

26 C. Drechsel-Grau and D. Marx, *Angewandte Chemie International Edition*, 2014, **53**, 10937–10940.

27 S. Fritsch, R. Potestio, D. Donadio and K. Kremer, *J. Chem. Theory Comput.*, 2014, **10**, 816–824.

28 J. A. Hayward and J. R. Reimers, *J. Chem. Phys.*, 1997, **106**, 1518–1529.

29 CPMD, *Copyright IBM Corp 1990-2008*, 1997-2001, Copyright MPI für Festkörperforschung Stuttgart.

30 N. Troullier and J. L. Martins, *Phys. Rev. B*, 1991, **43**, 1993–2006.

31 J. P. Perdew, K. Burke and M. Ernzerhof, *Phys. Rev. Lett.*, 1996, **77**, 3865–.

32 A. D. Becke, *Phys. Rev. A*, 1988, **38**, 3098–3100.

33 C. Lee, W. Yang and R. G. Parr, *Phys. Rev. B*, 1988, **37**, 785–789.

34 S. Nosé, *The Journal of Chemical Physics*, 1984, **81**, 511–519.

35 W. G. Hoover, *Phys. Rev. A*, 1985, **31**, 1695–1697.

36 R. Car and M. Parrinello, *Phys. Rev. Lett.*, 1985, **55**, 2471–2474.

37 G. J. Martyna, D. J. Tobias and M. L. Klein, *J. Chem. Phys.*, 1994, **101**, 4177–4189.

38 N. Marzari, A. A. Mostofi, J. R. Yates, I. Souza and D. Vanderbilt, *Rev. Mod. Phys.*, 2012, **84**, 1419–1475.

39 S. Kawada, *J. Phys. Soc. Jpn.*, 1979, **47**, 1850–1856.

40 G. P. Johari and S. J. Jones, *Proceedings of the Royal Society of London A: Mathematical, Physical and Engineering Sciences*, 1976, **349**, 467–495.